An Affirmative Action/Equal Opportunity Employer

LA-11338-MS

UC-32
Issued: August 1988

Sesame Equation of State Number 2293, Li

J. C. Boettger

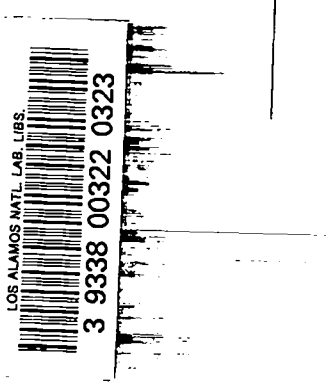

Los Alamos National Laboratory
Los Alamos, New Mexico 87545

SESAME EQUATION OF STATE NUMBER 2293, Li

by

J. C. Boettger

ABSTRACT

A new equation of state (EOS) for Li has been constructed and placed on the SESAME library as material number 2293. This new equation of state uses a cold curve obtained via electronic band structure calculations using the linear-muffin-tin-orbitals (LMTO) technique.

Recently, it was shown that the zero-temperature isotherm for crystalline Li exhibits a substantial shell structure effect due to a reordering of the 2s and 2p bands under pressure.[1] This shell structure effect does not appear in any of the current EOS's for Li on the SESAME library (material numbers 2290, 2291, and 2292). Since the EOS's for materials such as LiD may be formed by mixing the EOS's of their constituents,[2] it is important to have a high quality EOS for Li on the SESAME library. To this end we have produced a new EOS for Li which uses a cold curve in the compressed region obtained via electronic band structure calculations using the LMTO technique.[3] This EOS exhibits the desired shell structure effect in the cold curve and has been added to the SESAME library as material number 2293.

In the SESAME library, EOS's are partitioned into three terms for the pressure P and the internal energy E:

$$P(\rho,T) = P_c(\rho) + P_n(\rho,T) + P_e(\rho,T) \quad (1)$$

$$E(\rho,T) = E_c(\rho) + E_n(\rho,T) + E_e(\rho,T) \quad (2)$$

where ρ is the density and T is the temperature. The subscripts c, n, and e denote the contributions due to the cold curve (zero temperature isotherm), the nuclear motion, and the thermal electronic excitations. It is thus possible to treat each term independently using any desired model.

The nuclear and thermal electronic parts of 2293 were calculated with the program GRIZZLY,[4] using the CHART-JD[5] model for the nuclear term and the TFD model[6] for the thermal electronic term. In this part of the calculation six items of empirical input are required: the atomic mass (6.941),[7] the reference density (0.5331 gm/cc),[8] the Debye temperature (400 K),[8] the reference Gruneisen constant (0.88),[8] the cohesive energy (23.1 MJ/kg),[9] and the melting temperature (454 K).[9]

For compressions ranging from 0.9 to 20000, the cold curve was calculated via LMTO band structure calculations using the Kohn-Sham-Gaspar[10] local density approximation to the exchange-correlation. In these calculations, the crystal structure was assumed to be fcc. (The band structure calculations will be described in greater detail elsewhere.)[11] The resulting first principles cold curve was then adjusted empirically to ensure that the total pressure would be zero at room temperature for ρ = 0.5331 gm/cc. To achieve this, the pressures were uniformly shifted by -4.52 kbar and the energies were adjusted in a thermodynamically self-consistent manner by integration of the pressure correction. The cold curve in the expanded region was obtained from GRIZZLY by matching a Lennard-Jones type tail onto the compressed cold curve.[4] The parameter FACLJ (used by GRIZZLY to determine the exact shape of the tail) was adjusted to produce a critical temperature of about 3600 K (in rough agreement with material number 2291).

For comparative purposes, the most interesting of the earlier EOS's for Li in the SESAME library is material number 2292. That EOS was entirely calculated with GRIZZLY and uses the same nuclear and electronic models as 2293.[12] The only substantive difference between 2292 and 2293 is in the compressed cold curve, which was computed for 2292 using the CHUG model in GRIZZLY. In that model, the compressed cold curve is required to match any available Hugoniot data[13] and smoothly merge with a TFD cold curve in the large density limit. The advantage of this approach is that it ensures a good result along the principal Hugoniot, which is not necessarily true for other cold curve models.

In Fig.1, the room temperature isotherms for 2292 and 2293 are compared with experimental data.[14] It should be noted that there is a phase transition from the bcc structure to the fcc structure at a compression of 1.40.[14] This transition is not accounted for by either of the theoretical EOS's. However, the volume discontinuity at the transition is quite small[14] and the transition should be of little importance for this work. The apparent relatively large discontinuity in the pressure data shown in Fig.1 is most likely due to a buildup of strain in the sample as the transition is approached since no fluid medium was used in the experiment.[15] Immediately after the transition, the sample would once again be in hydrostatic equilibrium. For this reason, we feel that the data point at a compression of just over 1.3 should be ignored in our analysis.

In Fig.2, the principal Hugoniots for 2292 and 2293 are compared with LASL Hugoniot data.[13] Once again there is a phase transition within the range of the data. Here the melt transition occurs at a compression of about 1.3.[14] As in the case of the crystallographic phase transition discussed earlier, the melt transition is not accounted for by either of the theoretical EOS's.

Inspection of Figs. 1 and 2 reveals that 2293 is in slightly better agreement with experi-

ment except in the compression range from about 1.3 to about 1.65 (50 kbar < P < 150 kbar). In that range the pressures from 2293 are too large by no more than 5%. For both the room temperature isotherm and the Hugoniot, there would appear to be a lowering of the pressure in that range due to some effect which is not accounted for in the calculations. It is intriguing that this range of compressions is correlated with both the melt transition on the Hugoniot and the bcc to fcc transition on the room temperature isotherm. However, more work would be necessary to reveal whether or not these effects are actually related.

In Fig.3, the two EOS's are again compared with the LASL Hugoniot data (here in terms of the shock velocity U_s vs. the particle velocity U_p). In addition, the experimental adiabatic bulk sound speed[14] is given (solid circle) as the $U_p = 0$ limit of U_s. Again we see that 2293 is in slightly better agreement with experiment except for the three points which lie within the above noted compression range. (Here that range roughly corresponds to $1.5 < U_p < 3.5$ km/s.)

All of these experimental data taken together suggest that 2293 is in as good (if not better) agreement with the experiment as is 2292 for compressions up to 2.0. For higher compressions, the quality of the band structure calculations should steadily improve since the local-density approximation becomes more realistic as the density becomes more uniform. In contrast, the cold curve for 2292 beyond a compression of 2.0 is simply based on an interpolation formula which goes to the correct ultrahigh compression limit (TFD). It is also at these higher compressions that the shell structure begins to play a significant role.

In Fig.4, the room temperature isotherms for 2292 and 2293 are compared up to a compression of 10. Over this range of compressions the shell structure effect due to the reordering of the 2s and 2p states is evident in 2293. To exhibit this effect over an even greater range of compressions, Fig.5 shows the fractional deviation of the room temperature isotherms for 2293 and 2292 (P(2293)/P(2292) - 1). The relatively large deviation at normal

density is purely a result of a slight mismatch between the two zeros of pressure. It is clear that the shell structure is a significant effect throughout the range $3 < \rho/\rho_0 < 200$. At its greatest, this effect accounts for over 15% of the total pressure. For compressions greater than 200 (even beyond the range of Fig.5), the two isotherms agree to within the limits of precision for the two calculations. This is not surprising since the TFD cold curve is the ultrahigh compression limit for the band structure calculations.

In conclusion, it has been shown that material number 2293 in the SESAME library is in good agreement with existing experimental data (other than neglecting phase transitions). This new EOS also incorporates a major shell structure effect in the cold curve which is not accounted for in any previous SESAME EOS for Li. For this reason, 2293 should be viewed as the preferred EOS for calculations involving Li.

REFERENCES

1. W. G. Zittel, J. Meyer-ter-Vehn, J. C. Boettger, and S. B. Trickey, J. Phys. F: Met. Phys. 15, L247 (1985).

2. B. I. Bennett, Los Alamos National Laboratory, personal communication with author, March 1988. See material number 7245 on the SESAME library.

3. O. K. Anderson, Phys. Rev. B 12, 3060 (1975); O. K. Anderson and O. Jepsen, Physica (Utrecht) 91B, 317 (1977); H. L. Skriver, *The LMTO Method* (Springer, Berlin, 1984).

4. Joseph Abdallah, Jr., "User's Manual for GRIZZLY", Los Alamos National Laboratory report LA-10244-M (September 1984).

5. J. D. Johnson, Los Alamos National Laboratory, personal communications with author, March-September 1988.

6. GRIZZLY uses a version of CANDIDE for TFD modeling that was developed by D. A. Liberman and modified by J. D. Johnson. See also R. D. Cowan and J. Ashkin, Phys. Rev. 105, 144 (1957).

7. N. W. Ashcroft and N. D. Mermin, *Solid State Physics* (Holt, Rinehart, and Winston, 1976).

8. C. A. Swenson, Phys. Rev. B 31, 1150 (1985).

9. K. A. Gschneidner, Solid State Phys. 16, 276 (1964).

10. W. Kohn and L. J. Sham, Phys. Rev. 140, A1133 (1965); R. Gaspar, Acta Phys. Hung. 3, 263 (1954).

11. J. C. Boettger and R. C. Albers, to be published.

12. J. C. Boettger, unpublished notes on SESAME material number 2292.

13. S. P. Marsh, editor, *LASL Shock Hugoniot Data* (U. C. Press, 1980).

14. B. Olinger and J. W. Shaner, Science 219, 1071 (1983).

15. B. Olinger, Los Alamos National Laboratory, phone conversation with author, April 1988.

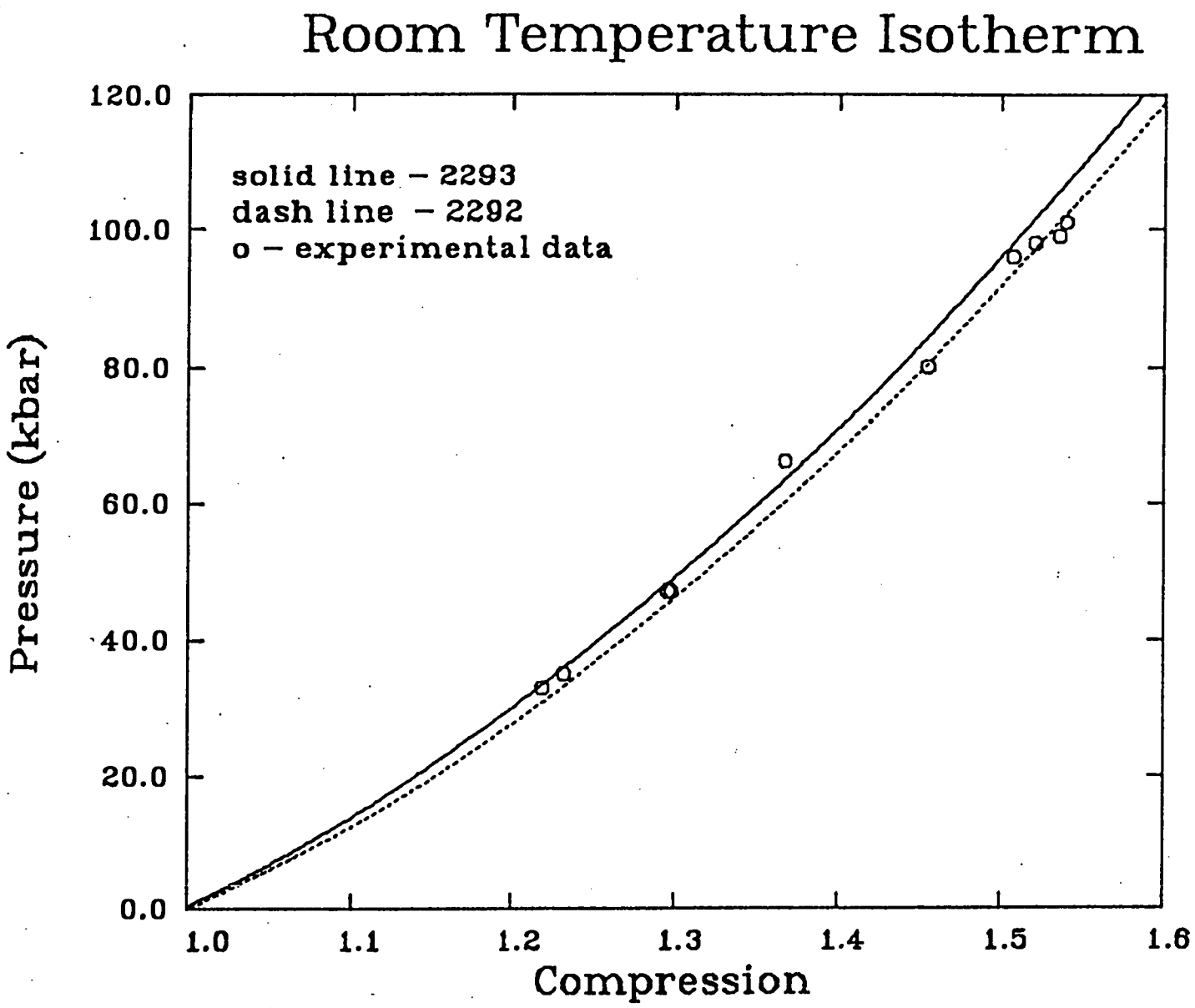

Fig. 1. Room temperature isotherms for material numbers 2292 (dashed line) and 2293 (solid line) compared with experimental data from Ref. 14.

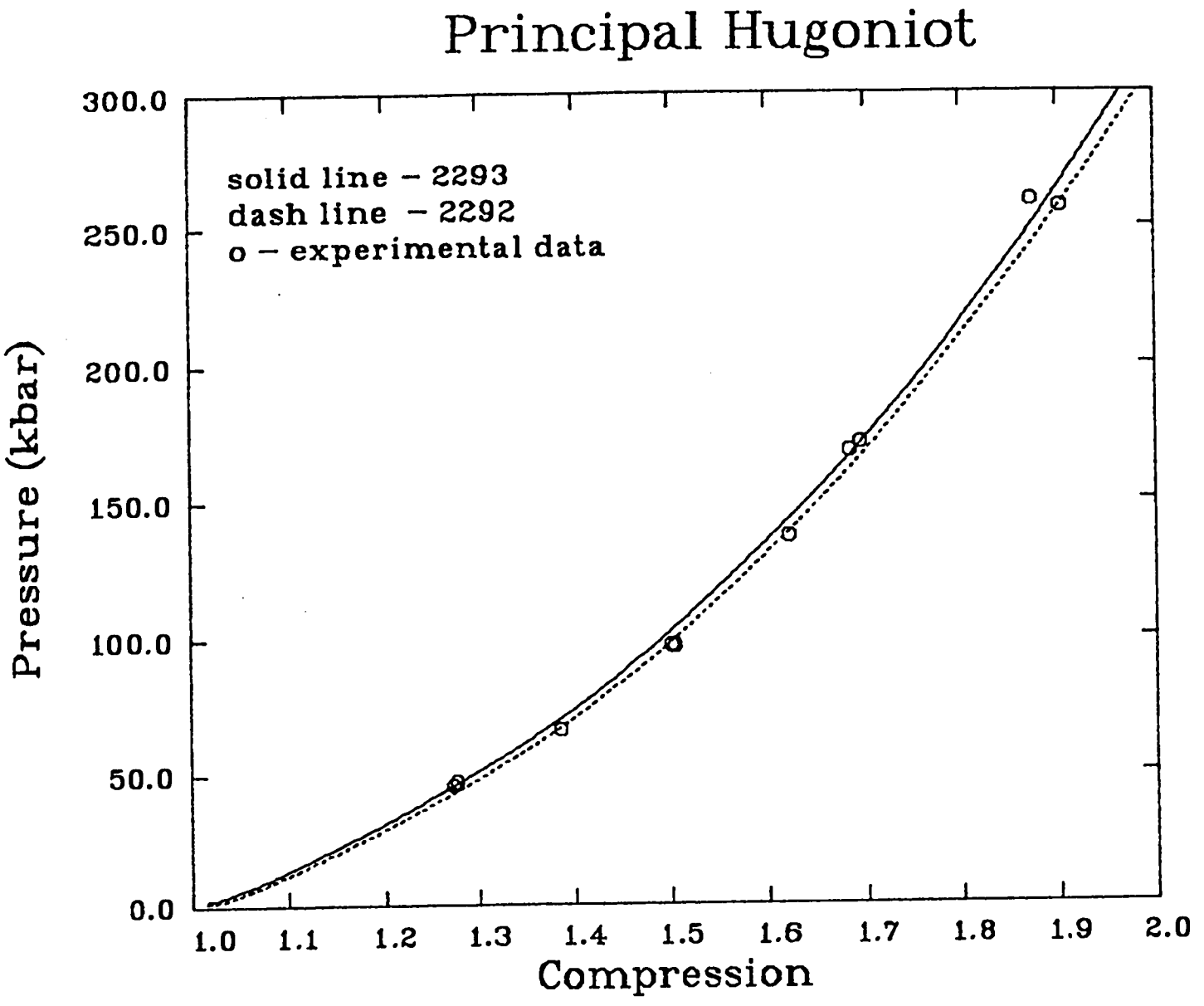

Fig. 2. Principal Hugoniots for material numbers 2292 (dashed line) and 2293 (solid line) compared with experimental data from Ref. 13.

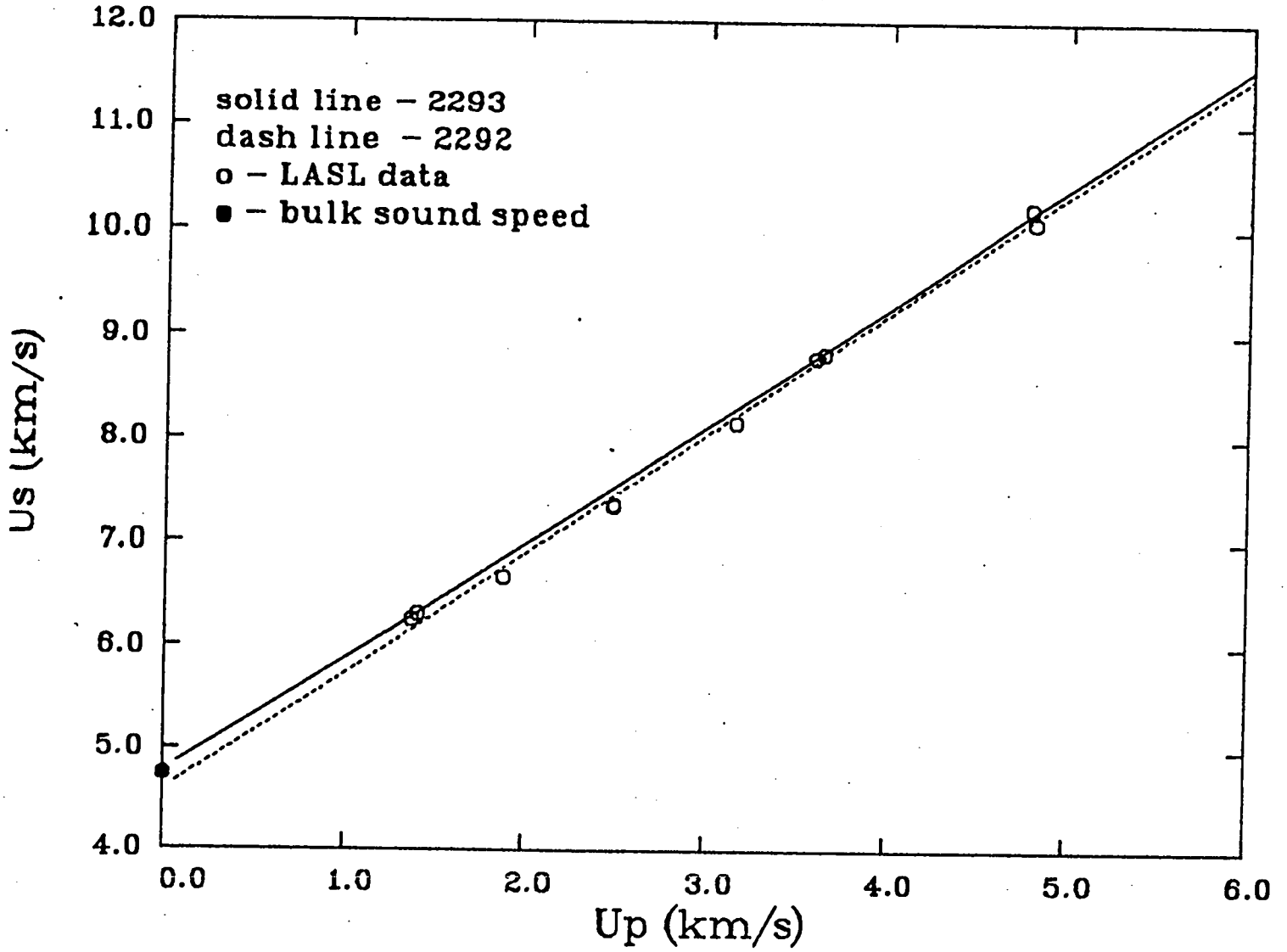

Fig. 3. Same as Fig. 2, except the data is in U_S vs. Up form. The solid circle is the bulk sound speed taken from Ref. 14.

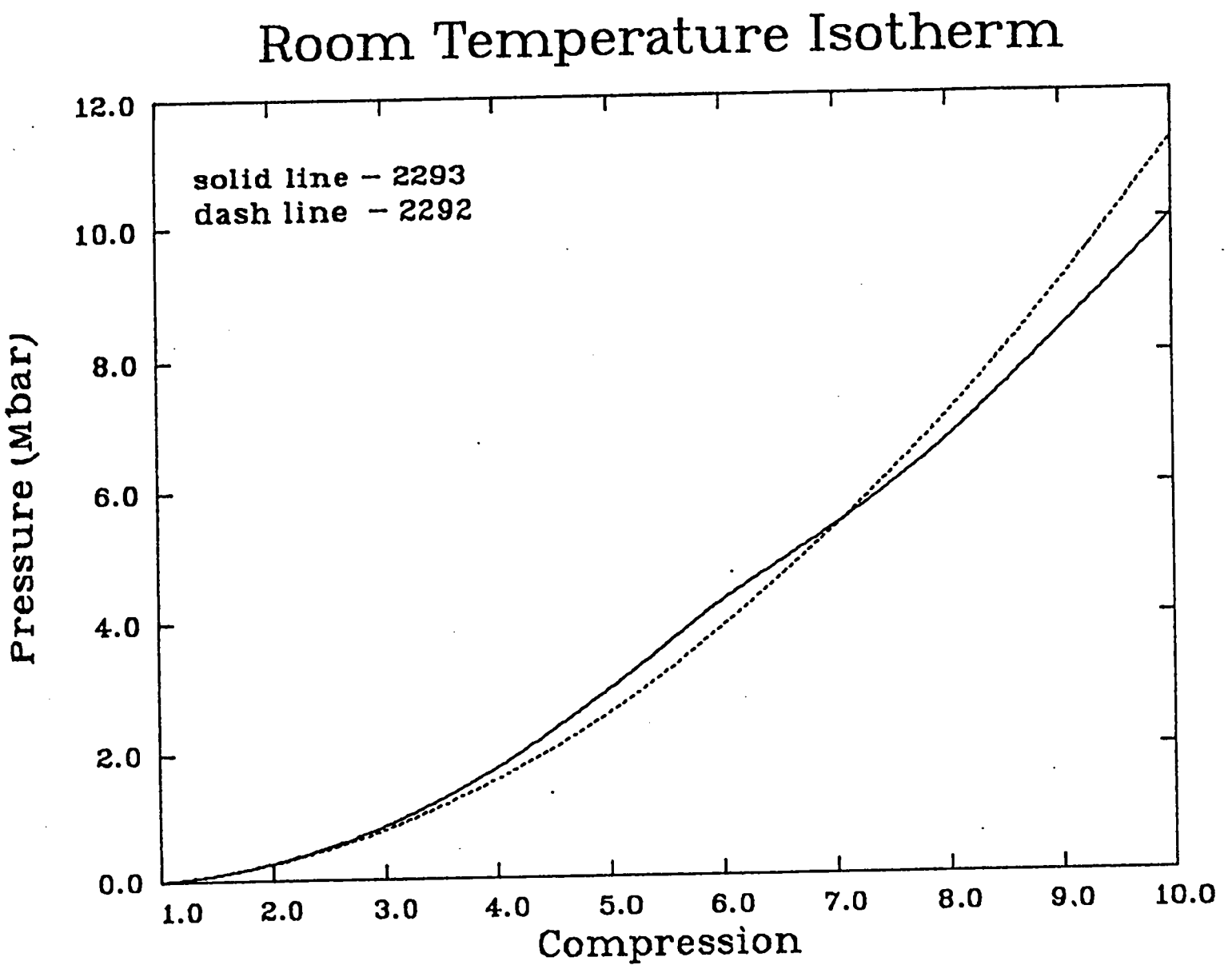

Fig. 4. Room temperature isotherms of 2292 (dashed line) and 2293 (solid line) for compressions up to 10.

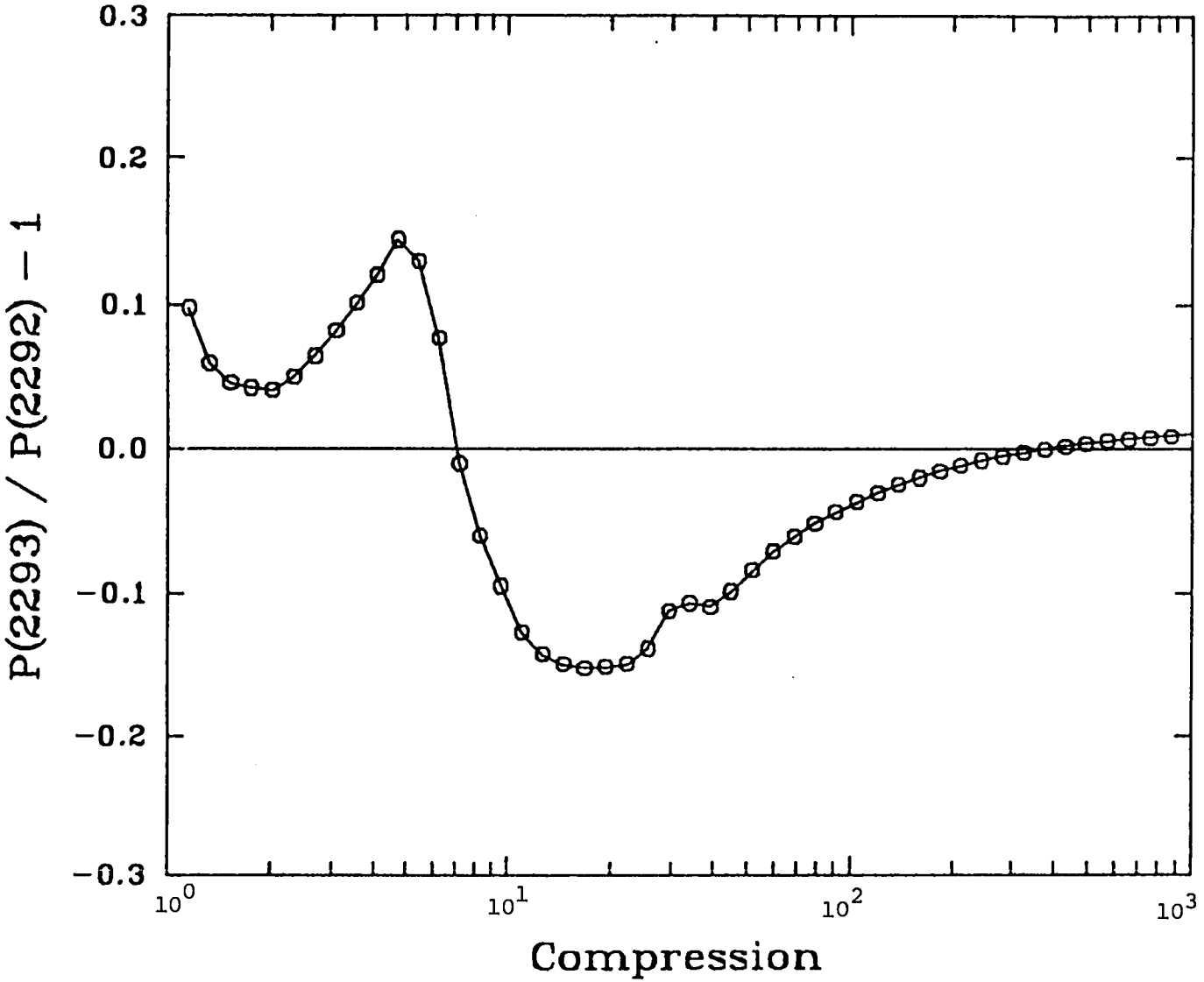

Fig. 5. Fractional deviation of 2293 from 2292 as a function of compression.

Printed in the United States of America
Available from
National Technical Information Service
US Department of Commerce
5285 Port Royal Road
Springfield, VA 22161

Microfiche (A01)

Page Range	NTIS Price Code	Page Range	NTIS Price Code	Page Range	NTIS Price Code	Page Range	NTIS Price Code
001-025	A02	151-175	A08	301-325	A14	451-475	A20
026-050	A03	176-200	A09	326-350	A15	476-500	A21
051-075	A04	201-225	A10	351-375	A16	501-525	A22
076-100	A05	226-250	A11	376-400	A17	526-550	A23
101-125	A06	251-275	A12	401-425	A18	551-575	A24
126-150	A07	276-300	A13	426-450	A19	576-600	A25
						601-up*	A99

*Contact NTIS for a price quote.

Los Alamos National Laboratory
Los Alamos, New Mexico 87545